International Journal of Information, Control and Computer Sciences
ISSN: 2517-9942
Vol:13, No:9, 2019

Pressure-Detecting Method for Estimating Levitation Gap Height of Swirl Gripper

Kaige Shi, Chao Jiang, Xin Li

***Abstract*—**The swirl gripper is an electrically activated noncontact handling device that uses swirling airflow to generate a lifting force. This force can be used to pick up a workpiece placed underneath the swirl gripper without any contact. It is applicable, for example, in the semiconductor wafer production line, where contact must be avoided during the handling and moving of a workpiece to minimize damage. When a workpiece levitates underneath a swirl gripper, the gap height between them is crucial for safe handling. Therefore, in this paper, we propose a method to estimate the levitation gap height by detecting pressure at two points. The method is based on theoretical model of the swirl gripper, and has been experimentally verified. Furthermore, the force between the gripper and the workpiece can also be estimated using the detected pressure. As a result, the nonlinear relationship between the force and gap height can be linearized by adjusting the rotating speed of the fan in the swirl gripper according to the estimated force and gap height. The linearized relationship is expected to enhance handling stability of the workpiece.

***Keywords*—**Swirl gripper, noncontact handling, levitation, gap height estimation.

I. Introduction

CONTACT handling of a workpiece often leads to surface scratching and static electricity. In the manufacturing process of thin and fragile products, such as silicon wafers, solar cell pieces, and glass panels, each product is handled frequently during repeated loading and unloading. Therefore, defect of product due to contact handling is common, which technically limits the productivity of the production line [1]. Furthermore, the thickness of the thin and fragile products is continuously reduced in order to economize materials and improve efficiency. For example, the thickness of silicon wafers will decrease to approximately 120 μm within the next 10 years [2]. This trend enhances the demand for noncontact handling devices. Many noncontact handling approaches have been proposed and proven effective [3]-[5], and the pneumatic noncontact grippers are the most common among them. The pneumatic grippers use airflow to generate a lifting force on the upper surface of the workpiece, such that the workpiece can be lifted and moved without solid contact. Bernoulli gripper, based upon the Bernoulli principle, is the most typical pneumatic noncontact gripper [6]-[11]. Recently developed vortex gripper, that takes advantage of vortex flow to achieve noncontact handling [12]-[15], is the other one. However, the pneumatic grippers are inefficient because they consume a large amount of compressed air. According to Li and Kagawa, when a Bernoulli gripper generates a 0.2 N lifting force, an compressed air flow of around 1.17×10^{-3} m^3/s (ANR) would be needed, which consumes nearly 90 W of electrical power to compress [16]. Then, they proposed an electrical noncontact gripper, namely swirl gripper, which is much more efficiency (less than 2 W for 0.2 N lifting force).

Kaige Shi and Xin Li are with the State Key Laboratory of Fluid Power and Mechatronic Systems, Zhejiang University, 38 Zheda-road, Hangzhou, Zhejiang, 310027, P.R.China (e-mail: shikg@zju.edu.cn, vortexdoctor@zju.edu.cn).

Chao Jiang is with the School of Mechanical Engineering, Zhejiang University, 38 Zheda-road, Hangzhou, Zhejiang, 310027, P. R. China (e-mail: jc31@163.com).

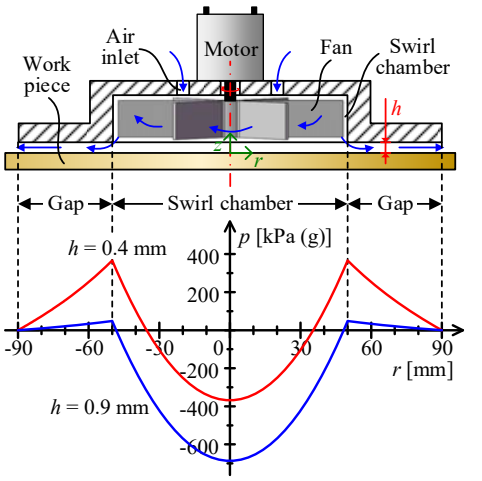

Fig. 1 Schematic and pressure distribution of swirl flow (ω =700 rad/s)

The schematic of the swirl gripper by Li and Kagawa is shown in Fig. 1. When the gripper works, the fan and the air in the swirl chamber rotates driven by the electrical motor.-Due to the centrifugal effect of the swirling air, as indicated by the pressure distribution in Fig. 1, a radially increasing pressure gradient forms in the chamber, which results in negative pressure in the central area. Meanwhile, the negative pressure in the swirl chamber sucks air from atmosphere through the air inlets on the top of the chamber. The intake air is discharged owing to centrifugal effect via the gap between the gripper and the workpiece. As shown in Fig. 1, the discharging airflow dominated by viscosity forms a positive pressure in the gap. When the gap height h between the gripper and the workpiece is small (e.g., h = 0.4 mm), as indicated by the red line in Fig. 1, the positive pressure in the gap is dominant, so the force F between the gripper and the workpiece is repulsive (see the red circle in Fig. 2(a)). When the gap height h is large (e.g., h = 0.9 mm), the force F yields to the negative pressure in the swirl chamber, so it becomes an attractive force that can lift the workpiece. Because the force F for a constant rotating speed ω

is a function of h as shown by the grey line in Fig. 2 (a), it can be treated as a fictitious spring between the gripper and the workpiece (see Fig. 2 (b)). The stiffness of the spring must be positive to ensure stable levitation of the workpiece, but F would decrease with h when h is large according to the F–h curves in [16], [17]. In practical applications of the noncontact gripper, the workpiece can only be stably lifted in the positive slope region of F–h curve, so the fictitious spring model is always valid.

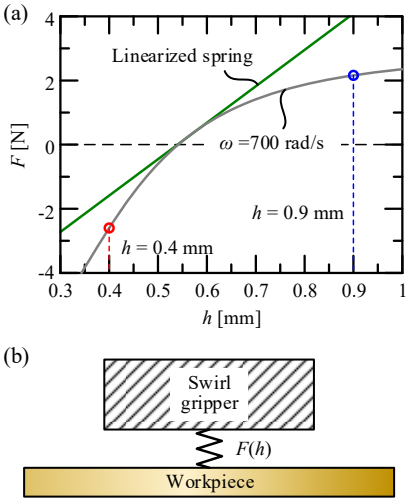

Fig. 2 F–h curve and fictitious spring model. (a) F–h curves for constant ω and linearized spring. (b) Fictitious spring model

In fact, the fictitious spring model can also be applied to pneumatic noncontact grippers since they have similar F–h curves [12]-[15], [18]-[20]. Previous study of noncontact grippers mainly focuses on the magnitude of the lifting force, while less attention has been paid to the character of the fictitious spring (i.e., the positive slope part of the F–h curve) of the gripper, which, in fact, is important for handling thin and fragile workpieces [21]. A relatively large gap height is desired in order to avoid collision between workpiece and gripper when they move with a downward acceleration. However, the levitation gap height depends on the stiffness of the fictitious spring, and is difficult to detect due to noncontact characteristic of the gripper. Furthermore, when the workpiece and gripper move with an upward acceleration, the gap height would increase, and the spring stiffness would decrease due to its nonlinearity. This might result in fall of the workpiece. Therefore, a linearized spring indicated by the green line in Fig. 2 (a) would be preferred.

In this article, a theoretical model of the swirl gripper will be built, based on which a method to estimate the gap height by detecting pressure at two points will be proposed. Additionally, the force can be estimated according to the detected pressures using similar method with Li and Kagawa [17]. After obtaining real-time force and gap height, the rotating speed of the fan can be adjusted simultaneously, such that the nonlinearity spring stiffness under a constant rotating speed can be compensated, and the fictitious spring can be a linearized.

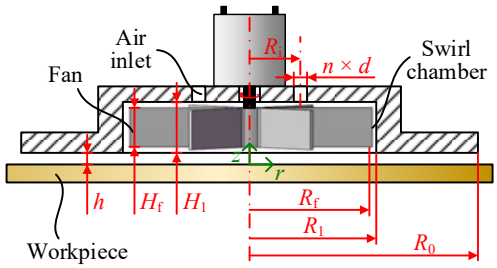

Fig. 3 Geometry of swirl gripper

TABLE I
GEOMETRIC PARAMETERS OF THE TESTED GRIPPER

R_0 [mm]	R_1 [mm]	H_1 [mm]	R_f [mm]	H_f [mm]	R_i [mm]	n [-]	d [mm]
90	50	20	49	16	20	4	6

II. THEORETICAL MODELING

A. Airflow in Swirl Chamber

The geometry of the swirl gripper is shown in Fig. 3, and the geometric parameters of the tested gripper are listed in Table I. Firstly, we model the swirl airflow in the swirl chamber ($0 < r < R_1$) from a fluid mechanics perspective. Due to the centrifugal effect of the swirl airflow, a radially increasing pressure gradient forms in the swirl chamber, such that the pressure in the central region is lower than on the periphery. It is assumed that the high-speed rotation causes the tangential velocity component of the air to dominate other velocity components and viscous effects so that the air motion equation can be simplified as

$$\frac{\rho {u_\alpha}^2}{r} = \frac{\partial p}{\partial r} \tag{1}$$

where p is the pressure, r is the radial position, ρ is the air density, and u_α is the tangential velocity. Furthermore, because the swirl airflow is driven by the fan, the tangential velocity u_α can be considered to be ωr, in which ω is the rotating speed of the fan. Therefore, (1) can be rewritten as

$$\rho \omega^2 r = \frac{\partial p}{\partial r} \tag{2}$$

Integrating (2) leads to

$$p(r) = \frac{1}{2}\rho\omega^2\left(r^2 - {R_1}^2\right) + p_1 \tag{3}$$

where R_1 is the radius of the swirl chamber, and p_1 is the pressure at $r = R_1$. The above equation suggests a parabolic pressure distribution in the swirl chamber, which has been experimentally verified in [16], [17].

Because the air inlets locate in the central region of the swirl chamber ($r = R_i$), the inlet pressure p_i is usually below atmospheric pressure and can be calculated using (3)

$$p_i = p_1 - \frac{1}{2}\rho\omega^2\left({R_1}^2 - {R_i}^2\right)$$

The total volume flow rate of the inlet air Q can be solved as

a function of p_i [22].

$$Q = nC_d \frac{\pi d^2}{4} \sqrt{\frac{-2p_i}{\rho}} \quad (5)$$

where n is the number of the air inlets, and C_d is coefficient of discharge depending on the geometry of the inlets.

The experimental setup in Fig. 4 was used to measure Q for various p_i. A plate with a small pressure tap and an air outlet was placed under the swirl gripper with zero gap height. A vacuum pump was used to create a negative pressure in the swirl chamber. The negative pressure in the chamber can be changed by adjusting the power of the vacuum pump. Because the fan did not rotate, the pressure in the chamber could be regarded as constant and was detected by a pressure sensor (±1 kPa, Nagano Keiki) via the small pressure tap. Meanwhile, the flow rate was measured using a flow meter (FD-A250, Keyence Corporation). The experimental result is plotted in Fig. 5 using blue triangles. Meanwhile, the red line represents theoretical curve based on (5) for $C_d = 0.5$. It can be seen that (5) can well predict Q for various p_i.

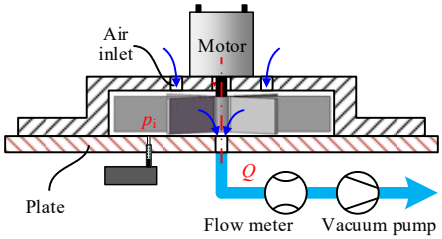

Fig. 4 Experimental setup for measuring flow rate

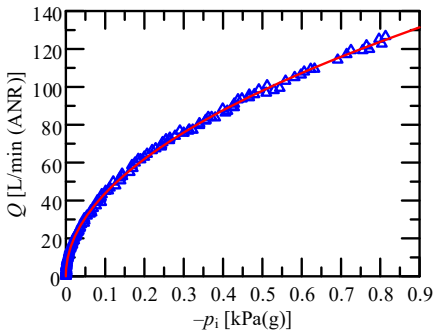

Fig. 5 Flow rate Q against p_i

B. Airflow in Gap

The air entering the swirl chamber rotates in the chamber, and is finally discharged into atmosphere through the annular thin gap ($R_1 < r < R_0$) between the gripper and workpiece. Because the height of the gap is usually very small, the airflow in the gap is dominated by viscosity, and can be treated as Stokes flow. Furthermore, the tangential velocity of the air is assumed to decelerate to zero soon after accessing the gap. Hence, only the radial velocity is considered, and the air motion equation is

$$\frac{\partial p}{\partial r} = \mu \frac{\partial^2 u_r}{\partial z^2} \quad (6)$$

The distribution of u_r in z direction can be assumed parabolic for viscous gap flow [22]

$$u_r = \frac{3Q}{\pi r h^3} \cdot z(h - z) \quad (7)$$

Substituting (7) into (6) and integrating it

$$p(r) = \frac{6\mu Q}{\pi h^3} \ln \frac{R_0}{r} \quad (8)$$

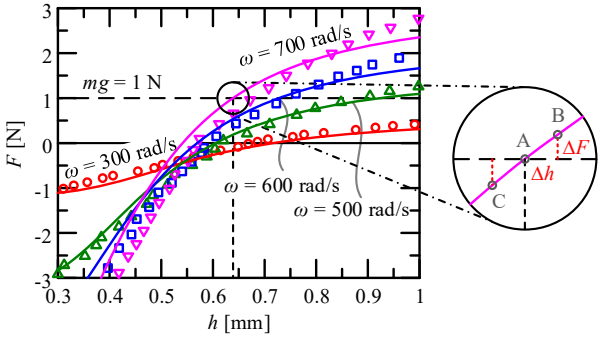

Fig. 6 F–h curves for ω = 300, 500, 600, and 700 rad/s

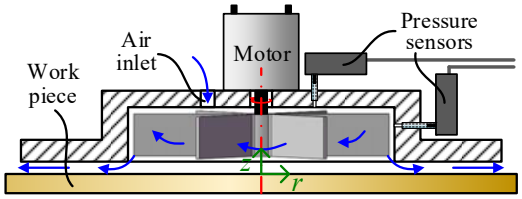

Fig. 7 Swirl gripper with pressure sensors

The pressure at $r = R_1$ thus can be obtained

$$p_1 = \frac{6\mu Q}{\pi h^3} \ln \frac{R_0}{R_1} \quad (9)$$

It has been noticed that, for a constant Q, p_1 is inversely proportional to the cube of h.

C. F–h Curve

Since the pressure distribution in the swirl chamber ($0 < r < R_1$) and in the gap ($R_1 < r < R_0$) has been given in (3) and (8), respectively, the force F between the gripper and the workpiece can be obtained by integrating $-p(r)$ over the area of $0 < r < R_0$

$$F = \frac{1}{4}\pi\rho\omega^2 {R_1}^4 - \frac{3\mu Q}{h^3}\left({R_0}^2 - {R_1}^2\right) \quad (10)$$

in which Q can be solved by combining (4), (5), and (9)

$$Q = \frac{\sqrt{\left(\frac{6\mu}{\pi h^3}\ln\frac{R_0}{R_1}\right)^2 + \left(\frac{4\rho\omega}{\pi n C_d d^2}\right)^2 \left({R_1}^2 - {R_i}^2\right)} - \frac{6\mu}{\pi h^3}\ln\frac{R_0}{R_1}}{\rho\left(\frac{4}{\pi n C_d d^2}\right)^2} \quad (11)$$

The theoretical F–h curves for various ω are plotted in Fig. 6, together with experimental data measured using the setup and method in the appendix. The theoretical results are in accordance with experimental results, verifying the theoretical model. It can be seen that F increases monotonously with h for a constant ω, which means the workpiece can levitate stably underneath the gripper. For example, as shown in Fig. 6, a workpiece weighting 1 N would levitate at point A without external disturbance. However, when external disturbance (e.g., accelerated movement of the workpiece and gripper) is applied, the workpiece may deviate from point A. When the workpiece deviates downward by Δh to point B, F increases by ΔF simultaneously. The increased F provides a restoring force and raises the workpiece towards point A. Otherwise, when the workpiece deviates upward to point C, F decreases, and the restoring force pulls the workpiece downward. The stability of the system is determined by the stiffness of the fictitious spring (i.e., $\Delta F/\Delta h$). A relatively large stiffness is desired to ensure the stability of the system. A negative stiffness would surely make the system unstable, while a small stiffness may fail to provide a large enough restoring force to overcome external disturbances.

Unfortunately, the stiffness of the fictitious spring varies with h, which further depends on the weight of the workpiece. Therefore, it would be helpful to obtain the actual value of h. Furthermore, the gap height h itself plays a crucial role in safe handling of the workpiece, because a small h increases the chance of collision between the workpiece and the gripper. In the next section, a method to estimate h will be proposed based on the theoretical model in this section.

III. Estimation of Levitation Gap Height

A. Proposed Method

Equation (9) implies that the gap height h can be reflected by p_1, which can be easily detected using a pressure sensor. However, the flow rate Q also affects p_1. To solve Q, (5) should be utilized. Substituting (5) into (9) leads to the following equation

$$h_e(p_i, p_1) = \left(1.5nC_d d^2 \mu \ln\frac{R_0}{R_1}\sqrt{\frac{2}{\rho}}\right)^{1/3} \cdot \frac{(-p_i)^{1/6}}{{p_1}^{1/3}} \qquad (12)$$

The first part of the expression of the estimated gap height h_e is a constant for a given gripper, while the second part includes p_i and p_1, which vary during the operation of the swirl gripper. Therefore, as shown in Fig. 7, two pressure sensors (±1 kPa, Nagano Keiki) are installed on the gripper to detect p_i and p_1. The pressure tap for p_i locates on the upper wall of the swirl chamber and at the same radius R_i with the air inlets. While the pressure tap for p_1 is on the cylindrical wall of the swirl chamber. The signals from the pressure sensors are transmitted to a microcontroller (Arduino Nano), and the microcontroller calculates h_e based on the detected pressures using (12). Due to the simple form of (12), the calculation can be implemented almost without delay.

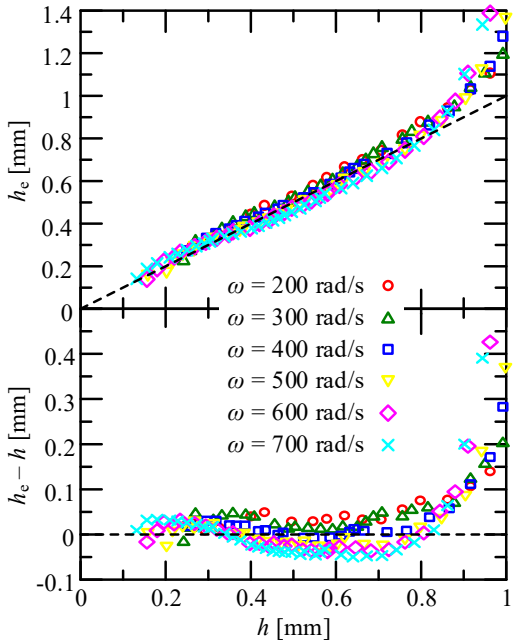

Fig. 8 Estimated gap height against actual value

B. Experimental Verification

In order to verify the method to estimate gap height, the following experiment has been conducted. Firstly, the swirl griper with pressure sensors was fixed on the setup in the appendix. Then, the rotating speed of the fan was set to a constant. The gap height h was adjusted by turning the feeding bolt in the setup. For each tested position, the reading from the laser meter was taken as the actual gap height h, while the result calculated by the microcontroller was recorded as h_e. The same procedure was repeated for ω = 200, 300, 400, 500, 600, and 700 rad/s. The experimental results have been plotted in Fig. 8. It can be seen that, in the region of $h < 0.8$ mm, h_e can track the change of h pretty well regardless of change in ω, and the error is within 0.08 mm, whereas, in the region of $h > 0.8$ mm, h_e is significantly larger than the actual value of h. The reason for this overestimation is that: the estimating method is based on the theoretical model of the swirl gripper, which treats the flow in the gap as Stokes flow and neglects its tangential velocity component. When h is large, the inertial effect of the discharging airflow in the gap, which is neglected in Stokes flow, can generate a radially increasing gradient of pressure according to Bernoulli principle [18], [19]. Furthermore, the tangential velocity in the swirl chamber is more likely to conduct to the gap when h is large, which contributes to the radially increasing gradient of pressure in the gap. As a result, the actual pressure p_1 at $r = R_1$ would be smaller than predicted by the theoretical model. According to (12), the value of p_1 approaches 0 as h increases. In this case, a small decrease in p_1 would lead to a large increase in h_e.

IV. Linearization of F–H Curve

Since the gap height can be estimated using the proposed method, F–h curve can be changed by adjusting the rotating

speed of the fan according to real-time h_e, such that it can be linearized. However, a feedback of F is needed to adjust ω. Li and Kagawa proposed pressure-distribution methods for estimating lifting force of the swirl gripper, in which F can be estimated based on either rotating speed and a single point pressure or two pressure points [17]. Here, we adopt similar method to estimate F. Substituting (4) and (9) into (10) gives:

$$F_e(p_i, p_1) = \frac{\pi {R_1}^4 (p_1 - p_i)}{2({R_1}^2 - {R_i}^2)} - \frac{\pi({R_0}^2 - {R_1}^2)p_1}{2\ln(R_0/R_1)} \quad (13)$$

By using (13), the estimated lifting force F_e can be obtained according to detected p_i and p_1.

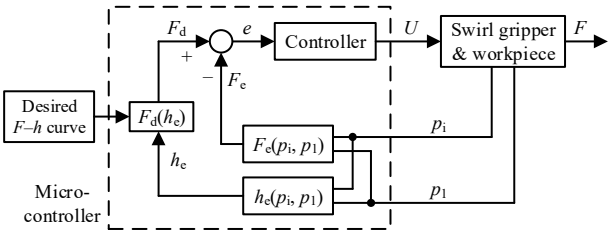

Fig. 9 System to achieve desired F–h curve

The system shown in Fig. 9 is used to achieve a desired F–h curve. The desired F–h curve is inputted to the microcontroller in advance. When the swirl gripper works, the microcontroller collects the signal from the pressure sensors and calculates Fe and he using (13) and (12), respectively. After that, the desired force Fd is obtained according to he and the desired F–h curve, while Fe is taken as the actual F. A controller based on PID algorithm is used to calculate the voltage U applied to the motor of the gripper according to the error between Fd and Fe. As a result, the output F can track the desired F–h curve.

Three desired F–h curves (F = 2700h – 1.89, F = 6000h – 3.78, and F = 9000h – 5.67) have been tested. The symbols in Fig. 10 show experimental data measured using the setup in the appendix, while the curves are the desired F–h curves. It can be seen that the experimental data locate close to the desired F–h curves in the region of h < 0.8 mm. However, F is significantly larger than desired when h > 0.8 mm. This is due to the significant overestimation of he in the region of h > 0.8 mm as shown in Fig. 8.

V. Conclusion

In this paper, we proposed a method to estimate levitation gap height of swirl gripper by detecting pressure at two points based on the theoretical model. During experimental verification of the method, it is found that the estimated gap height can well track actual value when the gap height is small, while significant overestimation occurs when the gap height becomes large. Furthermore, the detected pressure at two points can also be used to estimate the force between the gripper and the workpiece. Based on the estimated force and gap height, the F–h curve of the swirl gripper can be linearized using a microcontroller. The experimental result shows that the force of the gripper can track the desired F–h curve well when the gap height is small and can be correctly estimated.

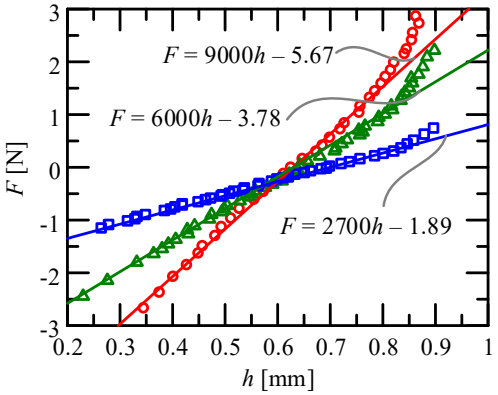

Fig. 10 Desired F–h curves and experimental results

Appendix. Experimental Setup and Method for Measuring Force and Gap Height

Fig. 11 shows the schematic and photograph of the setup used to measure the force F and gap height h. The tested gripper is fixed on the upper base via three sets of pins and pin clamps. To make the gripper parallel to the plate, the gripper is placed on the plate with the pin clamps loose, after which the pins extend to the upper base and are clamped. The plate is fixed on the shaft of an air guide with high linear precision, such that the shaft and plate can slide back and forth along the air guide with high parallel precision and no friction. A force sensor (SBT674, SimBaTouch) lies at the other end of the shaft with its mounting head contacting with the shaft. Since there is no friction between the shaft and the air guide, the force F can be obtained by subtracting the measured force from the weight of the plate and shaft. Moreover, the force sensor is installed on a slider; therefore, by turning the feeding bolt, the force sensor, shaft and plate can move vertically together, and as a result, the gap height h can be changed. Meanwhile, a fixed laser displacement meter (HG-C1030, Panasonics) is used to detect the position of the shaft, from which h can be obtained. By changing h continuously and recording F and h simultaneously, the relationship between F and h (i.e., the F–h curve) can be measured.

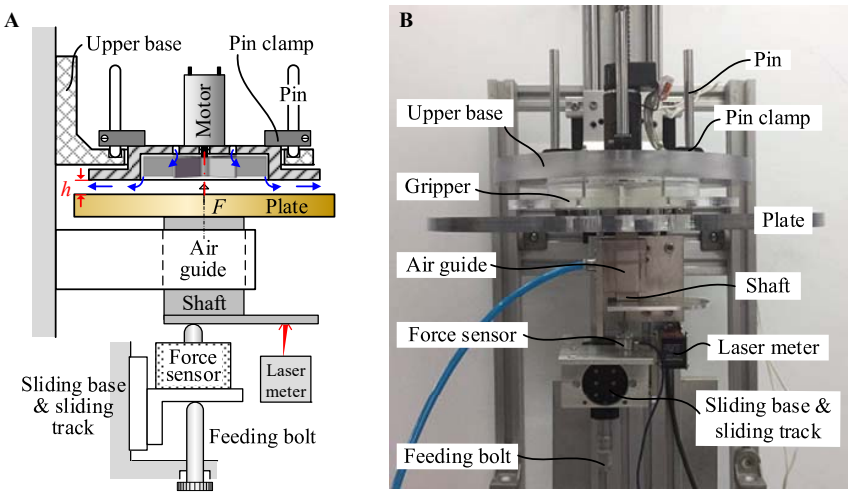

Fig. 11 Experimental setup for measuring force and gap height (A) Schematic (B) Photograph

ACKNOWLEDGMENT

This work is supported by the National Natural Science Foundation of China (Nos. U1613203 and 51375441) and the Fundamental Research Funds for the Central Universities (No. 51221004).

REFERENCES

[1] K. Reddig, "Overview of automation in the photovoltaic industry," *Photovolt. Int.,* vol. 4, pp. 18-29, 2009.
[2] T. Giesen *et al.*, "Advanced production challenges for automated ultra-thin wafer handling," presented at the 27th Eur. Photovoltaic Sol. Energy Conf. Exhib., Frankfurt, Germany, 2012.
[3] E. H. Brandt, "Levitation in Physics," *Science,* vol. 243, no. 4889, pp. 349-355, Jan 1989, doi: 10.1126/science.243.4889.349.
[4] J. A. Paivanas and J. K. Hassan, "Air Film System for Handling Semiconductor Wafers," *Ibm Journal of Research and Development,* vol. 23, no. 4, pp. 361-375, 1979 1979.
[5] V. Vandaele, P. Lambert, and A. Delchambre, "Non-contact handling in microassembly: Acoustical levitation," *Precision Engineering-Journal of the International Societies for Precision Engineering and Nanotechnology,* vol. 29, no. 4, pp. 491-505, Oct 2005, doi: 10.1016/j.precisioneng.2005.03.003.
[6] X. F. Brun and S. N. Melkote, "Modeling and Prediction of the Flow, Pressure, and Holding Force Generated by a Bernoulli Handling Device," *Journal of Manufacturing Science and Engineering-Transactions of the Asme,* vol. 131, no. 3, Jun 2009, Art no. 031018, doi: 10.1115/1.3139222.
[7] X. F. Brun and S. N. Melkote, "Analysis of stresses and breakage of crystalline silicon wafers during handling and transport," *Solar Energy Materials and Solar Cells,* vol. 93, no. 8, pp. 1238-1247, Aug 2009, doi: 10.1016/j.solmat.2009.01.016.
[8] S. Davis, J. O. Gray, and D. G. Caldwell, "An end effector based on the Bernoulli principle for handling sliced fruit and vegetables," *Robotics and Computer-Integrated Manufacturing,* vol. 24, no. 2, pp. 249-257, Apr 2008, doi: 10.1016/j.rcim.2006.11.002.
[9] G. Dini, G. Fantoni, and F. Failli, "Grasping leather plies by Bernoulli grippers," *Cirp Annals-Manufacturing Technology,* vol. 58, no. 1, pp. 21-24, 2009 2009, doi: 10.1016/j.cirp.2009.03.076.
[10] F. Erzincanli, J. M. Sharp, and S. Erhal, "Design and operational considerations of a non-contact robotic handling system for non-rigid materials," *International Journal of Machine Tools & Manufacture,* vol. 38, no. 4, pp. 353-361, Apr 1998, doi: 10.1016/s0890-6955(97)00037-0.
[11] B. R. Rawal, V. Pare, and K. Tripathi, "Development of noncontact end effector for handling of bakery products," *International Journal of Advanced Manufacturing Technology,* vol. 38, no. 5-6, pp. 524-528, Aug 2008, doi: 10.1007/s00170-007-1166-x.
[12] X. Li, K. Kawashima, and T. Kagawa, "Analysis of vortex levitation," *Experimental Thermal and Fluid Science,* vol. 32, no. 8, pp. 1448-1454, Sep 2008, doi: 10.1016/j.expthermflusci.2008.03.010.
[13] X. Li, S. Iio, K. Kawashima, and T. Kagawa, "Computational Fluid Dynamics Study of a Noncontact Handling Device Using Air-Swirling Flow," *Journal of Engineering Mechanics-Asce,* vol. 137, no. 6, pp. 400-409, Jun 2011, doi: 10.1061/(asce)em.1943-7889.0000237.
[14] X. Li, M. Horie, and T. Kagawa, "Study on the basic characteristics of a vortex bearing element," *International Journal of Advanced Manufacturing Technology,* vol. 64, no. 1-4, pp. 1-12, Jan 2013, doi: 10.1007/s00170-012-4372-0.
[15] L. Xin, W. Zhong, T. Kagawa, H. Liu, and G. Tao, "Development of a Pneumatic Sucker for Gripping Workpieces With Rough Surface," *Ieee Transactions on Automation Science and Engineering,* vol. 13, no. 2, pp. 639-646, Apr 2016, doi: 10.1109/tase.2014.2361251.
[16] X. Li and T. Kagawa, "Development of a new noncontact gripper using swirl vanes," *Robotics and Computer-Integrated Manufacturing,* vol. 29, no. 1, pp. 63-70, Feb 2013, doi: 10.1016/j.rcim.2012.07.002.
[17] X. Li, M. Horie, and T. Kagawa, "Pressure-Distribution Methods for Estimating Lifting Force of a Swirl Gripper," *Ieee-Asme Transactions on Mechatronics,* vol. 19, no. 2, pp. 707-718, Apr 2014, doi: 10.1109/tmech.2013.2256793.
[18] X. Li and T. Kagawa, "Theoretical and Experimental Study of Factors Affecting the Suction Force of a Bernoulli Gripper," (in English), *Journal of Engineering Mechanics,* Article vol. 140, no. 9, p. 11, Sep 2014, Art no. 04014066, doi: 10.1061/(asce)em.1943-7889.0000774.
[19] K. Shi and X. Li, "Optimization of outer diameter of Bernoulli gripper," *Experimental Thermal and Fluid Science,* vol. 77, pp. 284-294, Oct 2016, doi: 10.1016/j.expthermflusci.2016.03.024.
[20] K. Shi and X. Li, "Experimental and theoretical study of dynamic characteristics of Bernoulli gripper," *Precision Engineering-Journal of the International Societies for Precision Engineering and Nanotechnology,* vol. 52, pp. 323-331, Apr 2018, doi: 10.1016/j.precisioneng.2018.01.006.
[21] D. Liu, W. Liang, H. Zhu, C. S. Teo, K. K. Tan, and Ieee, "Development of a Distributed Bernoulli Gripper for Ultra-thin Wafer Handling," in *IEEE International Conference on Advanced Intelligent Mechatronics (AIM)*, Munich, Germany, 2017.
[22] B. R. Munson, D. F. Young, T. H. Okiishi, and W. W. Huebsch, *Fundamentals of Fluid Mechanics* 6th ed. 2009.